

Anthropogenic Warming Impacts on California Snowpack During Drought

Neil Berg and Alex Hall

Corresponding Author Information:

Neil Berg
nberg@atmos.ucla.edu

Dept. of Atmospheric and Oceanic Sciences
University of California, Los Angeles
Math Sciences Building 7229

ABSTRACT

1
2
3 Sierra Nevada climate and snowpack is simulated during the period of extreme drought from
4 2011 to 2015 and compared to an identical simulation except for the removal of 20th century
5 anthropogenic warming. Anthropogenic warming reduced average snowpack levels by 25%,
6 with mid-to-low elevations experiencing reductions between 26-43%. In terms of event
7 frequency, return periods associated with anomalies in 4-year April 1 SWE are estimated to have
8 doubled, and possibly quadrupled, due to past warming. We also estimate effects of future
9 anthropogenic warmth on snowpack during a drought similar to that of 2011 – 2015. Further
10 snowpack declines of 60-85% are expected, depending on emissions scenario. The return periods
11 associated with future snowpack levels are estimated to range from millennia to much longer.
12 Therefore, past human emissions of greenhouse gases are already negatively impacting statewide
13 water resources, and much more severe impacts are likely to be inevitable.

14

15 **1. Introduction**

16 California recently experienced an epic 4-year (2011/12 – 2014/15) drought, with extremely
17 warm temperatures and low precipitation throughout the state (e.g. Swain et al. 2014,
18 AghaKouchak et al. 2014). The drought manifested itself in record-breaking dry soils (Griffin
19 and Anchukaitis 2014, Williams et al. 2015, Robeson 2015) and has led to significant
20 agricultural damage (Howitt et al. 2014) alongside rapid depletion of groundwater resources
21 (Famiglietti et al. 2014). The precipitation deficit driving the drought can be primarily
22 understood through natural variability (Seager et al. 2015). While recent multi-year low
23 precipitation totals are extreme, there is no evidence that historical California precipitation

24 exhibits any negative trend (Berg et al. 2015, Seager et al. 2015). Future precipitation is also
25 expected to increase somewhat over California (e.g. Neelin et al. 2013), lending further support
26 to the notion that anthropogenic precipitation changes have likely not influenced the recent
27 drought. Anthropogenic temperature changes, on the other hand, have repeatedly been invoked
28 to explain the severity of record dry soils across California (Griffin and Anchukaitis 2014,
29 Williams et al. 2015, Shukla et al. 2015, Cheng et al. 2016).

30
31 Snow is another hydrologic variable influenced by warming. In 2015, April 1 snow water
32 equivalent (SWE) in the Sierra Nevada reached a low unprecedented within the past 500 years
33 (Belmecheri et al. 2015), coinciding with the warmest California winter on record
34 (<http://www.ncdc.noaa.gov/sotc/national/201503>). This alarming statistic begs the question: how
35 have anthropogenic temperature changes influenced California snowpack during the 4-year
36 drought? Addressing this question is a focus here, building on two prior studies. Shukla et al.
37 (2015) find that the ranking of the 2013/14 Sierra Nevada snowpack was below the 2nd percentile
38 for the 1916 – 2012 period. They also show that if 2013/14 temperatures had resembled any
39 prior historical year, there is a 90% chance that 2013/14 SWE would have ranked above the 2nd
40 percentile. So the unusual warmth of 2013/14 (the second warmest winter on record behind
41 2014/15, <http://www.ncdc.noaa.gov/sotc/national/201403>) likely contributed to the low
42 snowpack conditions of that year. Mao et al. (2015) also analyze the role of anthropogenic
43 temperatures on 2012-2014 April 1 SWE over the Sierra Nevada by simulating snowpack
44 conditions when daily minimum temperature trends across the cold-season (November-March)
45 and warm-season (April-October) are removed from the forcing data. Their results suggest that

46 recent warming more than doubled the return period of the 3-year 2012-2014 average April 1
47 SWE over the Sierra Nevada.

48
49 This study advances these prior results in two respects. First, we include observed and simulated
50 2014/15 snowpack totals in our analyses, providing for a more comprehensive assessment of the
51 role of past anthropogenic temperature change in the low Sierra Nevada snowpack during the
52 entire 4-year drought. Second, we also examine effects on snowpack if the drought had unfolded
53 under the much more severe warming occurring at the end of the 21st century under enhanced
54 anthropogenic forcing. This is accomplished by performing a series of experiments simulating
55 2011/12 – 2014/15 snowpack levels when subjected to future conditions derived from
56 downscaled regional climate projections. We explore the full range of plausible greenhouse gas
57 forcing scenarios, allowing for an assessment of the inevitability of snowpack change during
58 future drought conditions.

59

60 **2. Data and Methods**

61 **2a. Coupled WRF-NoahMP simulation**

62 To quantify the role of anthropogenic warming in the record-setting low 2011/12 – 2014/15
63 California snowpack, we perform regional climate simulations using version 3.5 of the Weather
64 Research and Forecast model (WRF, Skamarock et al. 2008) and the Noah land surface model
65 with multiparameterization options (NoahMP, Niu et al. 2011) in both coupled and uncoupled
66 (or offline) frameworks. A January 1980 – June 2015 baseline climatology is first simulated in
67 coupled mode. The coupled baseline simulation is also used to drive offline simulations
68 described in Section 2b. The coupled simulation uses two domains (Fig. 1a), D01 (27 km) and

69 D02 (9 km), to resolve California’s Sierra Nevada topography and relevant fine-scale climatic
70 features (e.g. snow albedo feedback, land-sea breeze). Boundary conditions for the coupled
71 baseline simulation are supplied by 6-hourly North American Regional Reanalysis output
72 (Mesinger et al. 2006). Multiple parameterization packages were tested and the optimal
73 configuration was shown to accurately simulate spatial and temporal patterns of observed Sierra
74 Nevada SWE (c.f. Fig. S2 in Sun et al. 2016). Additional information on the coupled model
75 configuration can be found in Section S1. Its performance in simulating California hydrology is
76 further detailed in Walton et al. 2016, Sun et al. 2016, and Schwartz et al. 2016.

77

78 **2b. Uncoupled WRF-NoahMP simulations**

79 We next create an uncoupled version of the January 1980 – June 2015 baseline land surface
80 conditions. This is achieved by forcing the offline NoahMP model with 3-hourly outputs of 2 m
81 air temperature, surface pressure, shortwave and longwave radiation, 10 m wind speed, 10 m
82 wind direction, precipitation, and relative humidity from the aforementioned 9 km (D02) coupled
83 baseline simulation. For computational efficiency, only grid cells in D02 that experience over 10
84 mm of 1980 – 2015 annual-mean SWE are simulated (Fig. 1b). Evaluation of simulated SWE
85 from this offline “reference” experiment is found in Section 2c.

86

87 Following the reference experiment, five additional experiments, each spanning June 2011 –
88 June 2015, are executed where temperature inputs to the offline model are perturbed by various
89 amounts. First, a “natural” experiment is performed where the monthly warming that has arisen
90 over the past century is removed at each time step in a given month. This experiment estimates
91 how 2011/12 – 2014/15 snowpack totals would have evolved in the absence of past warming.

92 Warming is computed from two observational products, the 2°x2° GISS Surface Temperature
93 Analysis spanning January 1880 – May 2015 (Hansen et al. 2010, available at
94 <http://data.giss.nasa.gov/gistemp/>) and the 5°x5° Climatic Research Unit temperature database
95 spanning January 1850 – May 2015 (Jones et al. 2012, available at
96 <http://www.cru.uea.ac.uk/cru/data/temperature/#sciref>). For each month, 1880 – 2015 (or 2014
97 for months June – December) time series of temperature anomalies with respect to 1880 – 1919
98 are averaged across California grid cells within each data set. Warming for a given month is
99 then calculated as the difference between two 35-year averages, a recent climate of 1981 – 2015
100 (or 1980 – 2014 for months June through December) minus a past climate of 1880 – 1914.
101 Averaged across the two data sets, this yields monthly warming (units °C) of 1.33 (January),
102 1.30 (February), 1.24 (March), 0.73 (April), 1.11 (May), 1.11 (June), 1.0 (July), 0.95 (August),
103 1.46 (September), 1.12 (October), 0.37 (November), and 0.27 (December). Very similar values
104 are obtained with different averaging periods and through trend analysis (Section S2, Table S1).
105 Also note that global climate models (GCMs) on average estimate that anthropogenic forcings
106 have contributed to around 1°C annual warming by the start of the 21st century over North
107 America (c.f. Fig. 10.7, Bindoff et al. 2013), reasonably consistent with the above values. Thus
108 we interpret the “natural” experiment as representing a regional climate state that is identical to
109 that of 2011/12 – 2014/15, but without anthropogenic forcing.

110

111 Finally, we analyze how 2011/12 – 2014/15 snowpack responds to end-of-21st century projected
112 temperature increases with four future experiments corresponding to the Representative
113 Concentration Pathway (RCP) emissions scenarios (RCP2.6, RCP4.5, RCP6.0, and RCP8.5)
114 used in the IPCC Fifth Assessment Report (Van Vuuren et al. 2011). In these future experiments,

115 we rely on a hybrid downscaling framework to generate end-of-century monthly warming values
116 at 3 km resolution for all available GCMs and emissions scenarios over the Sierra Nevada
117 (Walton et al. 2016). The GCM-mean downscaled projection is computed for each scenario and
118 then coarsened to 9 km to match the resolution of the offline grid dimensions used in this study
119 (Fig. 1). For each grid cell in the offline simulations, we increase temperatures by month
120 according to its ensemble-mean change at the nearest grid cell in the 9 km downscaled projection.

121

122 **2c. Uncoupled model evaluation of SWE**

123 Here we evaluate simulated Sierra Nevada SWE from the reference experiment based on a
124 collection of 93 in-situ stations (red dots Fig. 1b) that recorded April 1 SWE from 1930 – 2015.
125 Data is provided by the California Department of Water Resources (CDWR, available at
126 <http://cdec.water.ca.gov/snow/current/snow/index.html>) and the National Resources
127 Conversation Service (NRCS, available at <http://www.wcc.nrcs.usda.gov/snow/>). Figure 2
128 compares time series of the observed station-average April 1 SWE and simulated values
129 averaged across grid cells nearest to the 93 station locations for the overlapping period of 1980 –
130 2015. Simulated output in this comparison has already been adjusted for the grid-to-point
131 elevation mismatch (Section S3, Figures S1, S2). Simulated climatological April 1 SWE is 696.6
132 mm, nearly equal to the average observed value of 690.4 mm. Standard deviations for the
133 simulated and observed time series are 333.6 and 324.0 mm, respectively. These very small
134 biases, indicates that WRF-NoahMP quite accurately simulates Sierra Nevada SWE compared to
135 observed data.

136

137 **3. Past and future anthropogenic warming impacts**

138 **3a. Elevational dependency**

139 Figure 3 compares September 2011 – June 2015 time series of daily SWE from the six offline
140 experiments averaged across grid cells in various elevation categories: all elevations (Fig. 3a),
141 high elevations (>2500 m, Fig. 3b), mid elevations (1500-2500 m, Fig. 3c), and low elevations
142 (<1500 m, Fig. 3d). Results are further summarized in Table 1. Focusing on the 4-snow year
143 (November – June) average, anthropogenic warming reduced 2011/12 – 2014/15 average annual
144 snowpack levels by 17.2 mm (25%) across all elevations and by 9.2 mm (10%), 19.7 mm (26%),
145 and 16.4 mm (43%) for the high, mid, and low elevations, respectively. Hence, snowpack at
146 mid-to-low elevations is much more affected by recent warming trends than snowpack at the
147 highest elevations.

148

149 Strong impacts to the mid elevations (also discussed in Sun et al. 2016) are particularly
150 noteworthy given that the mid-elevations encompass over 60% of the entire domain. In terms of
151 volumetric SWE (i.e. SWE multiplied by area), mid-elevations also dominate. The reference 4-
152 snow year average equals 0.357 km^3 over all elevations and 0.230 km^3 in just the mid elevations
153 (Fig. 3a,c). In the natural experiment, the corresponding values are 0.473 km^3 over all elevations
154 and 0.313 km^3 for the mid elevations (Fig. 3a,c). Thus, 0.116 km^3 (94 kAf) of additional total
155 snowpack would have resulted if anthropogenic warming had not occurred, 71% of which would
156 be found in mid-elevations. For perspective, 94 kAf of water is roughly twice the current annual
157 residential water demands for the city of San Francisco (~46 kAf, SFPUC 2014)

158

159 Projected 21st century warming applied to this recent period would diminish snowpack levels
160 even further. Under the least aggressive emission scenario of RCP2.6 (dark blue line, Fig. 3), 4-

161 year average snowpack levels are significantly reduced from the levels of the reference
162 experiment by 24.6 mm (47%) across the entire domain. However, estimates of recent global
163 greenhouse gas emissions (Le Quéré et al. 2015) show that RCP2.6 involves emissions
164 reductions that have not occurred since the RCP forcing scenarios were created in 2005. The
165 significant reductions associated with RCP2.6 in the coming decades are likewise unlikely to
166 occur. Thus we only consider RCP4.5, RCP6.0, and RCP8.5 to be the plausible forcing scenarios.
167 RCP4.5, which also involves emissions reductions over the coming decades, may be the most
168 realistic “mitigation” scenario. Under this scenario (light blue line, Fig. 3), total snowpack is
169 reduced by 31.9 mm or 60%. RCP8.5 is the scenario emissions have been tracking over the past
170 10 years, and will continue to track if emissions keep increasing at the same pace, and can be
171 considered a “business-as-usual” scenario. Under RCP8.5 (red line, Fig. 3), total snowpack is
172 reduced by 45.2 mm or 85%, and even high elevations become susceptible to large declines of
173 55.3 mm (67%). Nearly all snowpack is lost at mid and low elevations, with reductions
174 exceeding 90% for each category. Volumetric SWE declines by 0.305 km^3 (over 247 kAf)
175 between the reference and RCP8.5 simulations, over five times the annual residential usage in
176 San Francisco.

177

178 **3b. Event frequency**

179 We next quantify how return periods of simulated 4-year average (2012-2015) April 1 snowpack
180 levels change under current and future anthropogenic warming in Figure 4. Observed April 1
181 return periods of 4-year events are first computed using the 93 CDWR/NRCS station-average
182 data set. To minimize possible biases due to anthropogenic trends in the station data, we only
183 consider the first half of the observed time series, 1930-1970, when computing observed return

184 periods. These return periods are simply equal to the observed length of the sample size plus one
185 (i.e. 42 years) divided by the rank of the sorted running 4-year 1930-1970 SWE averages from
186 lowest to highest (grey triangles, Fig. 4). A normal distribution is then fitted to the set of
187 observed 4-year averages and corresponding fitted return periods are computed (black line).
188 Several distribution types were tested and the normal distribution proved to be the best fit. 95%
189 confidence intervals are obtained via a bootstrap-resampling technique (black dashed lines,
190 details in Section S4). 4-year average SWE from the six offline simulations are placed on the
191 fitted curve to estimate their return periods (colored dots, Fig. 4). Finally, the observed 2012-
192 2015 average is noted by a magenta dash-dot line.

193
194 The observed 2012 – 2015 station-average of 270.4 mm (magenta dash-dot line in Fig. 4) is by
195 far the lowest 4-year average on record (including 1971-2015, not shown). This very low 4-year
196 snowpack is matched by the “reference” WRF-NoahMP experiment, when model and
197 observational uncertainty are considered. (See Section S3 and Fig. S2 for details on the
198 calculation of these error bars.) For the longer return periods, the associated 95% confidence
199 level uncertainty is large, making it difficult to make precise statements about the return periods
200 of any individual SWE value when that value is very low. However, relative values may be
201 meaningful. For example, comparing the natural to the reference experiment, the return period is
202 roughly two to four times longer with anthropogenic warming than without.

203
204 Using output from the future warming experiments, we also provide estimates of the event
205 frequency of 2012 – 2015 snowpack levels when subjected to end-of-century warming. The
206 results are shown as dark blue (RCP2.6), light blue (RCP4.5), orange (RCP6.0), and red

207 (RCP8.5) dots in Fig. 4. Examining the plausible forcing scenarios (RCP4.5, RCP6.0 and
208 RCP8.5), it is evident that any additional warming applied to the already thin 2012 – 2015
209 snowpack yields almost incalculable return periods, from millennial time scales to much longer.
210 While future snowpack will likely be shaped by factors beyond just warming, our idealized
211 experiments suggest that a future 4-year period with precipitation characteristics like 2012 –
212 2015 would yield snowpack levels that cannot be reconciled with the snowpack statistics of the
213 historical record, no matter which plausible forcing scenario is chosen.

214

215 **4. Summary and Discussion**

216 Offline simulations reveal that observed century-scale warming exacerbated Sierra Nevada
217 snowpack loss significantly during 2011/12 – 2014/15. Across the region, warming reduced 4-
218 year average snowpack levels by 25%, with even greater relative losses concentrated in the mid
219 and low elevations. In terms of event frequency, warming has at least doubled, and perhaps
220 quadrupled, estimated return periods of the 2011/12 – 2014/15 4-year average April 1 snowpack.
221 While absolute values of the return periods are different, Mao et al. (2015) also found over a
222 doubling of return periods for 3-year (2012-2014) April 1 SWE events due to anthropogenic
223 warming. And while a period exactly like 2011/12 – 2014/15 will obviously not recur, droughts
224 like it surely will, and end-of-century anthropogenic warming applied to this time span results in
225 snowpack declines of 60-85% and estimated 4-year return periods range from millennial to much
226 longer time scales, no matter which realistic forcing scenario is chosen. In other words, when it
227 comes to snowpack, future drought will have no analog in the historical record.

228

229 These results corroborate recent findings of a clear link between anthropogenic warming and the
230 ongoing drought's severity (e.g. Griffin and Anchukaitis 2014, Williams et al. 2015). While
231 consecutive years of low precipitation lie at the origin of recently depleted snowpack levels (Mao
232 et al. 2015), this study suggests that California's water situation (Brown 2015) would not have
233 been so dire had anthropogenic warming not occurred. Moreover, we find that even with
234 significant emissions reductions, such as those of the RCP4.5 forcing scenario, future Sierra
235 Nevada-based water resources are expected to further diminish due to additional warmth. Going
236 forward, it is likely to become more difficult to satisfy municipal, agricultural, and ecological
237 water needs within a warmer climate, and clearly water will have to be managed very differently
238 during periods of extreme drought.

239

240

241 REFERENCES

242

243 AghaKouchak A., L. Cheng, O. Mazdoyasni, A. Farahmand (2014) Global Warming and
244 Changes in Risk of Concurrent Climate Extremes: Insights from the 2014 California Drought
245 *Geophysical Research Letters*, 41, 8847-8852, doi: 10.1002/2014GL062308.

246

247 Belmecheri, S., F. Babst, E. R. Wahl, D. W. Stahle, and V. Touret (2015) Multi-century
248 evaluation of Sierra Nevada snowpack. *Nature Climate Change*, doi:10.1038/nclimate2809.

249

250 Berg, N. and A. Hall (2015) Increased Interannual Precipitation Extremes over California under
251 Climate Change. *J. Climate*, **28**, 6324–6334. doi: <http://dx.doi.org/10.1175/JCLI-D-14-00624.1>

252

253 Bindoff, N.L., P.A. Stott, K.M. AchutaRao, M.R. Allen, N. Gillett, D. Gutzler, K. Hansingo, G.
254 Hegerl, Y. Hu, S. Jain, I.I. Mokhov, J. Overland, J. Perlwitz, R. Sebbari and X. Zhang (2013)
255 Detection and Attribution of Climate Change: from Global to Regional. In: Climate Change
256 2013: The Physical Science Basis. Contribution of Working Group I to the Fifth Assessment
257 Report of the Intergovernmental Panel on Climate Change [Stocker, T.F., D. Qin, G.-K. Plattner,
258 M. Tignor, S.K. Allen, J. Boschung, A. Nauels, Y. Xia, V. Bex and P.M. Midgley (eds.)].
259 Cambridge University Press, Cambridge, United Kingdom and New York, NY, USA.
260
261 Brown, E. G. J. (2015) Executive Order B-29-15 (Executive Department of California,
262 https://www.gov.ca.gov/docs/4.1.15_Executive_Order.pdf).
263
264 Boé, J., L. Terray, F. Habets, and E. Martin (2007) Statistical and dynamical downscaling of the
265 Seine basin climate for hydro-meteorological studies. *International Journal of*
266 *Climatology*, 27(12), 1643-1656.
267
268 Cheng L., M. Hoerling, A. AghaKouchak, B. Livneh, X. Quan (2016) How Has Human-
269 Induced Climate Change Affected California Drought Risk? *Journal of Climate* 29.1: 111-120.
270
271 Famiglietti, J. S. (2014) The global groundwater crisis. *Nature Climate Change*, 4, 945-948.
272 doi:10.1038/nclimate2425
273
274 Griffin, D., and K. J. Anchukaitis (2014), How unusual is the 2012–2014 California
275 drought?, *Geophys. Res. Lett.*, 41, 9017–9023, doi:[10.1002/2014GL062433](https://doi.org/10.1002/2014GL062433).

276

277 Gudmundsson, L., J. B. Bremnes, J. E. Haugen, and T. Engen-Skaugen (2012) Technical Note:
278 Downscaling RCM precipitation to the station scale using statistical transformations—a
279 comparison of methods. *Hydrology and Earth System Sciences*, 16(9), 3383-3390.

280

281 Hansen, J., R. Ruedy, M. Sato, and K. Lo (2010) Global surface temperature change, *Rev.*
282 *Geophys.*, **48**, RG4004, doi:10.1029/2010RG000345

283

284 Howitt, R., J. Medellin-Azuara, D. MacEwan, J. Lund, and D. A. Sumner (2014), Economic
285 analysis of the 2014 drought for California agriculture, UC Davis Cent. for Watershed Sci.,
286 Davis, Calif. [https://watershed.ucdavis.edu/files/biblio/DroughtReport_23July2014_0.pdf.]

287

288 Jones, P. D., D. H. Lister, T. J. Osborn, C. Harpham, M. Salmon, M. and C. P. Morice (2012)
289 Hemispheric and large-scale land surface air temperature variations: an extensive revision and an
290 update to 2010. *Journal of Geophysical Research* **117**, D05127, doi:10.1029/2011JD017139.

291

292 Le Quéré, C., et al. (2015): Global Carbon Budget 2014. *Earth System Science Data*, **7**: 47–85.
293 doi:10.5194/essd-7-47-2015.

294

295 Los Angeles Department of Water and Power (LADWP) (2010): Urban Water Management
296 Plan, 1-567, available at <http://www.water.ca.gov/urbanwatermanagement/2010uwmps/Los>
297 [Angeles Department of Water and Power/LADWP UWMP_2010_LowRes.pdf](http://www.water.ca.gov/urbanwatermanagement/2010uwmps/Los)

298

299 Mao, Y., B. Nijssen, and D. P. Lettenmaier (2015): Is climate change implicated in the 2013–
300 2014 California drought? A hydrologic perspective. *Geophys. Res. Lett.*, 42, 2805–2813.
301 doi:[10.1002/2015GL063456](https://doi.org/10.1002/2015GL063456).

302

303 Maurer, E. P. and D. Pierce (2014) Bias correction can modify climate model simulated
304 precipitation changes without adverse effect on the ensemble mean. *Hydro. Earth Sys. Sci.*, 18,
305 915-925.

306

307 Maurer, E. P., H. G. Hidalgo, T. Das, M. D. Dettinger, and D. R. Cayan (2010) The utility of
308 daily large-scale climate data in the assessment of climate change impacts on daily streamflow in
309 California. *Hydrology and Earth System Sciences*, 14(6), 1125-1138.

310

311 Meko, D. (1997) Dendrochromatic reconstruction with time varying prediction subsets of tree
312 indices. *J. Climate*, 10(4), 687-696.

313

314 Mesinger, F., G. DiMego, E. Kalnay, K. Mitchell, P. C. Shafran, W. Ebisuzaki, D. Jović, J.
315 Woollen, E. Rogers, E. H. Berbery, M. B. Ek, Y. Fan, R. Grumbine, W. Higgins, H. Li, Y. Lin,
316 G. Manikin, D. Parrish, and W. Shi (2006) North American Regional Reanalysis. *Bull. Amer.*
317 *Meteor. Soc.*, **87**, 343–360. doi: <http://dx.doi.org/10.1175/BAMS-87-3-343>

318

319 Neelin, J.D., Langenbrunner, B., J. E. Meyerson, A. Hall, and N. Berg (2013) California Winter
320 Precipitation Change under Global Warming in the Coupled Model Intercomparison Project
321 Phase 5 Ensemble. *J. Climate*, **26**, 6238–6256.

322 doi: <http://dx.doi.org/10.1175/JCLI-D-12-00514.1>
323
324 Niu, G.-Y., et al. (2011) The community Noah land surface model with multiparameterization
325 options (Noah-MP): 1. Model description and evaluation with local-scale measurements, *J.*
326 *Geophys. Res.*, 116, D12109, doi:[10.1029/2010JD015139](https://doi.org/10.1029/2010JD015139).
327
328 Robeson, S. M. (2015). Revisiting the recent California drought as an extreme
329 value. *Geophysical Research Letters*, 42(16), 6771-6779. doi:[10.1002/2015GL064593](https://doi.org/10.1002/2015GL064593).
330
331 San Francisco Public Utilities Commission (SFPUC) Water Resources Division (2014): Annual
332 Report Fiscal Year 2013-2014.
333 <http://www.sfwater.org/modules/showdocument.aspx?documentid=6543>
334
335 Schwartz, M., A. Hall, F. Sun, D. Walton, and N. Berg (2015) Significant end-of-21st-century
336 warming-driven advances in surface runoff timing in California's Sierra Nevada. *In Preparation*.
337
338 Seager, R., M. Hoerling, S. Schubert, H. Wang, B. Lyon, A. Kumar, J. Nakamura, and N.
339 Henderson (2015) Causes of the 2011 to 2014 California drought, *J. Clim.*, doi:[10.1175/JCLI-D-](https://doi.org/10.1175/JCLI-D-14-00860.1)
340 [14-00860.1](https://doi.org/10.1175/JCLI-D-14-00860.1), in press.
341
342 Shukla, S., M. Safeeq, A. AghaKouchak, K. Guan, and C. Funk (2015), Temperature impacts on
343 the water year 2014 drought in California. *Geophys. Res. Lett.*, 42, 4384–4393.
344 doi:[10.1002/2015GL063666](https://doi.org/10.1002/2015GL063666).

345

346 Skamarock W. C., J. B. Klemp, J. Dudhia, D. O. Gill, D. M. Barker, M. G. Duda, X.-Y. Huang,
347 W. Wang, and J. G. Powers (2008) A description of the Advanced Research WRF Version 3.
348 NCAR Tech. Note NCAR/TN-475+STR, June 2008, 125 pp.

349

350 Sun, F., A. Hall, M. Schwartz, N. Berg, and D. Walton (2016) Inevitable end-of-century loss of
351 spring snowpack over California's Sierra Nevada. *Submitted to Nature Climate Change*.

352

353 Swain, D. L., M. Tsian, M. Haugen, D. Singh, A. Charland, B. Rajaratnam, and N. S.
354 Diffenbaugh (2014) The Extraordinary California Drought of 2013/2014: Character, Context,
355 and the Role of Climate Change, *Bull. Amer. Meteor. Soc.*, 95 (9), S3-S7.

356

357 Thrasher, B., E. P. Maurer, C. McKellar, and P. B (2012) Technical Note: Bias correcting
358 climate model simulated daily temperature extremes with quantile mapping. *Hydrology and
359 Earth System Sciences*, 16(9), 3309-3314.

360

361 Van Vuuren et al. (2011). The representative concentration pathways: an overview. *Climatic
362 change*, 109, 5-31.

363

364 Walton, D., A. Hall, N. Berg, M. Schwartz, and F. Sun (2016) Incorporating snow albedo
365 feedback into downscaled temperature and snow cover projections for California's Sierra
366 Nevada. *J. Climate*, in press.

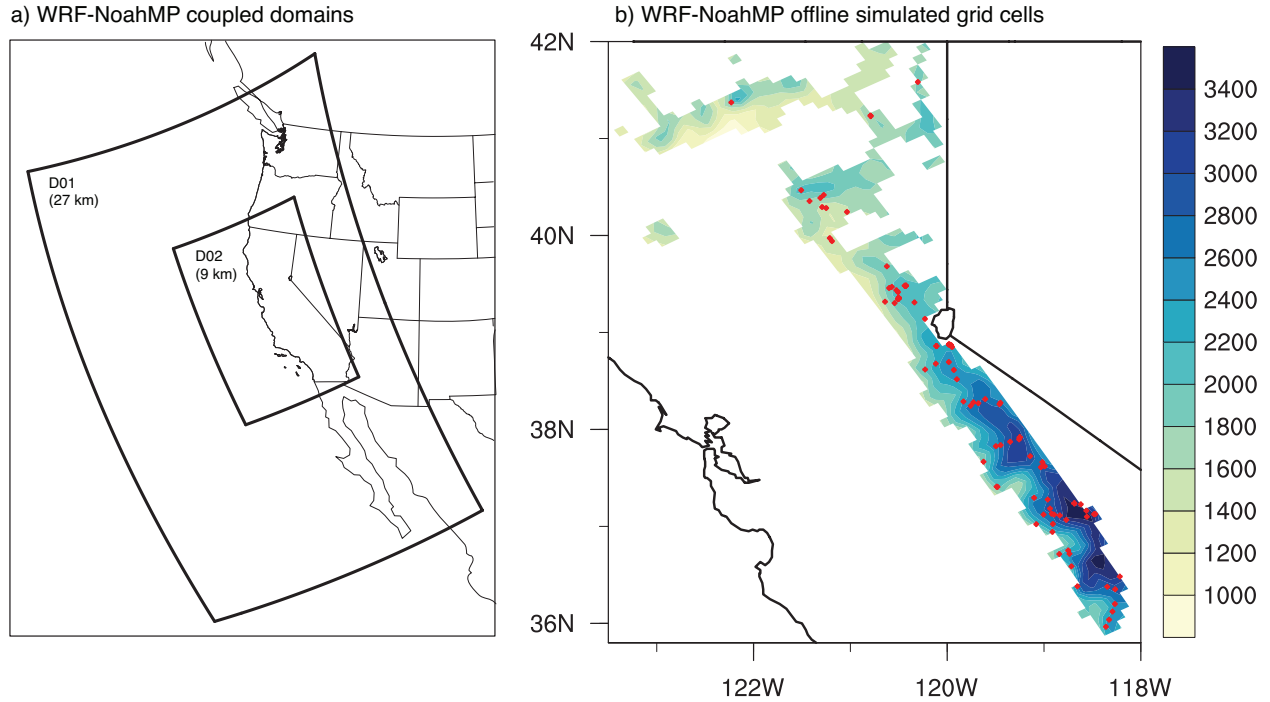
367

368
369
370
371
372
373
374
375
376
377
378
379
380
381
382
383
384
385
386
387
388
389
390

Williams, A. P., R. Seager, J. T. Abatzoglou, B. I. Cook, J. E. Smerdon, and E. R. Cook (2015) Contribution of anthropogenic warming to California drought during 2012–2014, *Geophys. Res. Lett.*, 42, 6819–6828, doi:[10.1002/2015GL064924](https://doi.org/10.1002/2015GL064924).

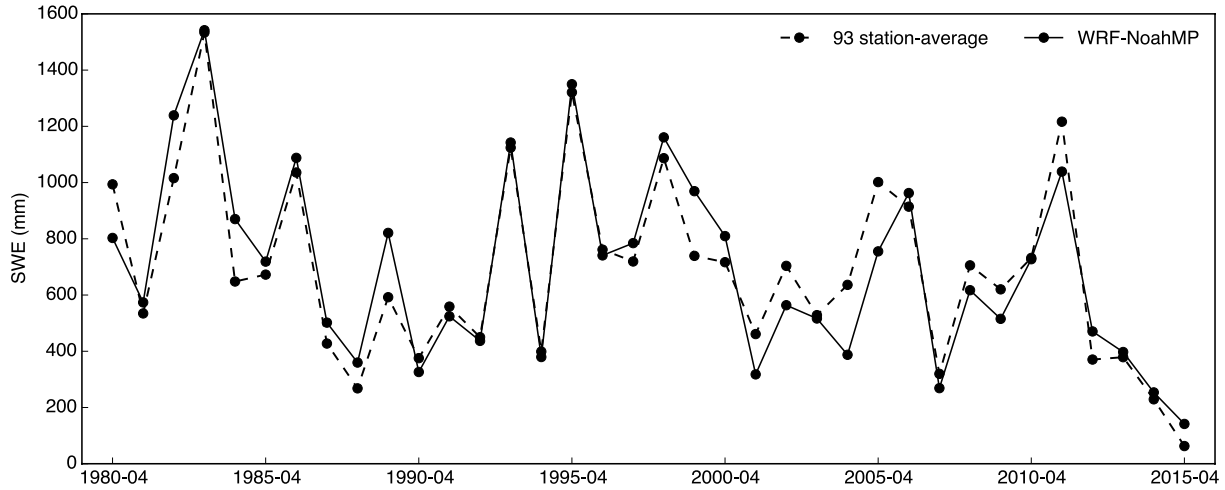
Wood, A. W., L. R. Leung, V. Sridhar, and D. P. Letenmaier (2004) Hydrologic implications of dynamical and statistical approaches to downscaling climate model outputs. *Climatic Change*, 62, 189-216.

391
392



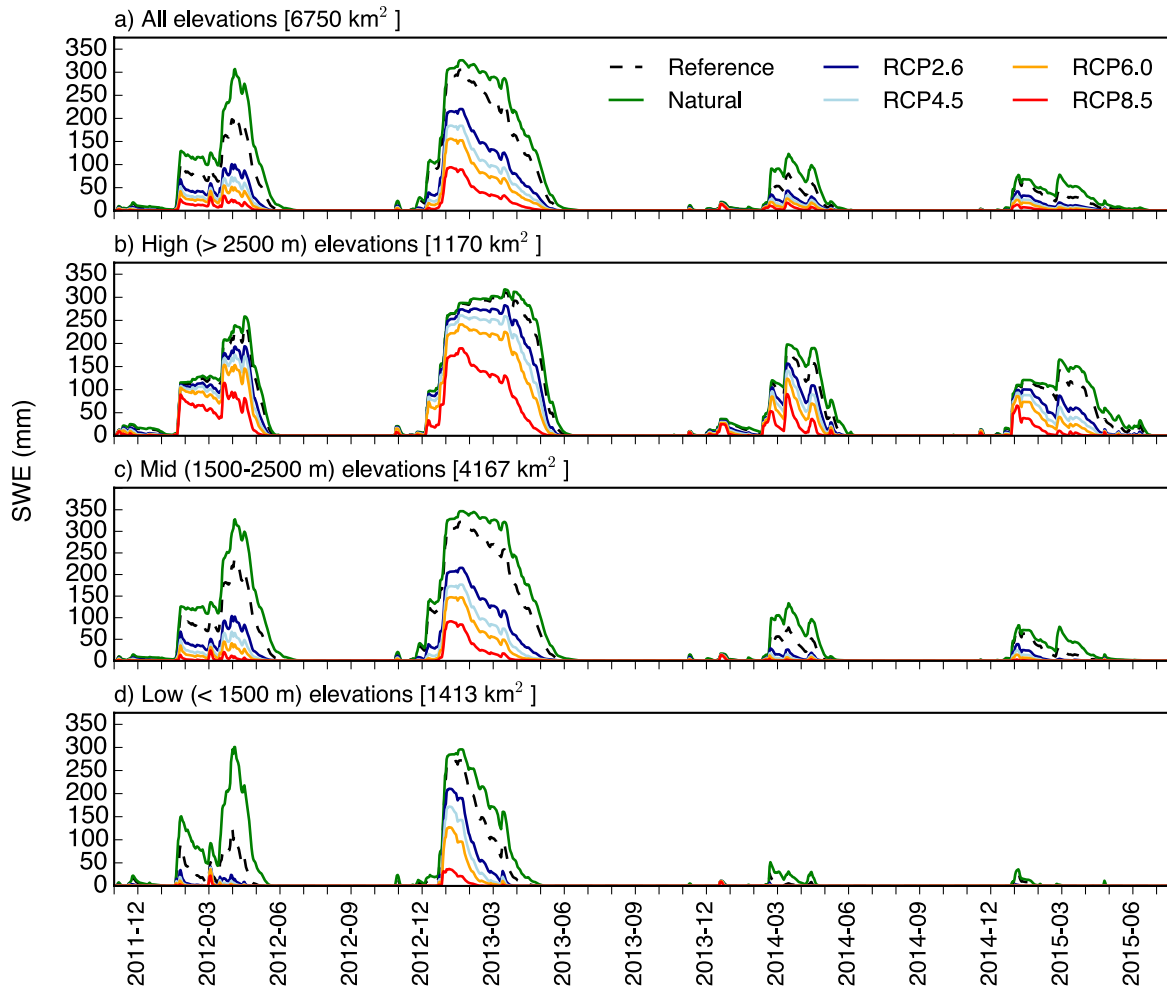
393
394 FIG 1. (a) Location of nested WRF-NoahMP coupled domains: D01 (27 km resolution) – D02 (9
395 km resolution). (b) 9 km resolution grid cells (750 total) selected for WRF-NoahMP offline
396 simulations, as they experience over 10 mm of annual SWE averaged across 1980 – 2015. Grid
397 cell elevation (unit m) is shaded according to the legend on the right. Locations of 93
398 CDWR/NRCS snowpack observations are overlaid as red dots.
399

400
401
402
403
404
405
406
407



408
 409
 410
 411
 412
 413
 414
 415

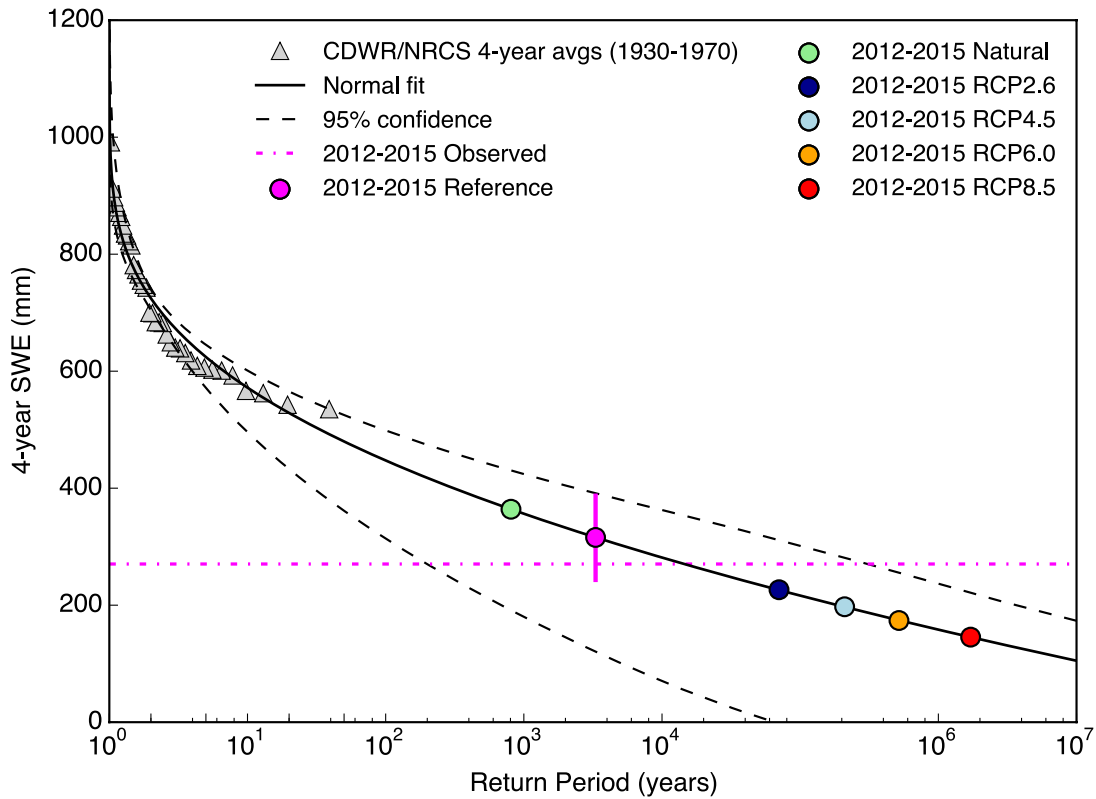
FIG 2. April 1 SWE (unit mm) according to the 93 station-averaged observations (dashed) and the average of the nearest grid cells to the 93 stations in the WRF-NoahMP reference simulation (solid) for the overlapping period of 1980 – 2015. Simulated output is corrected for grid-to-station elevation mismatch.



416
 417
 418
 419
 420
 421
 422
 423
 424
 425
 426
 427
 428
 429
 430
 431
 432
 433
 434
 435

FIG 3. September 2011 – June 2015 daily SWE (unit mm) according to the reference (black dashed), natural (green), RCP2.6 (dark blue), RCP4.5 (light blue), RCP6.0 (orange), RCP8.5 (red) simulations averaged over (a) all grid cells, (b) grid cells with elevations greater than 2500 m, (c) grid cells with elevations between 1500-2500 m, and (d) grid cells with elevations lower than 1500 m. The area of each elevation category is noted in the brackets.

436
437



438
439

FIG 4. Observed (1930-1970) return periods of 4-year averaged 93 CDWR/NRCS station-averaged April 1 SWE (grey triangles) and estimated return periods of corresponding simulated values (colored dots) using a normal fitted distribution (black line, 95% confidence intervals in black dashes). The observed 2012-2015 average April 1 SWE amount is shown in magenta dash-dot line. Error bars on the 2012-2015 simulated “reference” experiment (solid magenta line) are based on results in Figure S2a.

440
441
442
443
444
445
446
447
448
449
450
451
452
453
454
455
456
457

	Reference	Natural	RCP2.6	RCP4.5	RCP6.0	RCP8.5
All elevations	52.9	70.1	28.3	21.0	15.8	7.7
High elevations	82.0	91.2	65.0	56.3	46.9	26.7
Mid elevations	55.3	75.0	24.4	16.1	11.0	4.7
Low elevations	21.7	38.1	9.6	6.5	4.2	1.1

458
459
460
461
462

TABLE 1. Simulated 2011/12 – 2014/15 snow-year (November – June) average SWE (unit mm) across all elevations, high elevations (> 2500 m), mid elevations (1500-2500 m), and low elevations (< 1500 m) for each experiment. Data corresponds to time series in Figure 3.